A Phenomenological Model for Self-rippling Energy of Free Graphene Monolayer and Its Application

By

Bing Jie Wu

A thesis submitted in partial fulfillment of the requirements for the degree of

Master of Science

Department of Mechanical Engineering
University of Alberta

Abstract

Several candidate phenomenological expressions are studied for self-rippling energy that drives ripple formation of free single-layer graphene sheets. One phenomenological expression is admitted based on the stability criterion of periodic ripple mode, while all others are rejected because they cannot admit stable periodic ripple mode. The admitted phenomenological expression contains two terms: one quadratic term which acts like a compressive force and has a destabilizing effect, and another fourth-order term which acts like a nonlinear elastic foundation and has a stabilizing effect. The two associated coefficients depend on specific mechanism of self-rippling and can be determined based on observed wavelength and amplitude of ripple mode.

Based on the admitted expression, the effect of an applied force on ripple formation is studied. The present model predicts that the rippling can be controlled or even suppressed with an applied tensile force, or collapsed into narrow wrinkles (of deformed wavelengths down to around 2 nm) under an applied compressive force, and the estimated minimum tensile strain to suppress rippling is in remarkable agreement with some known data. Our results show that self-rippling energy dominates ripple formation of sufficiently long free graphene ribbons, although it cannot drive self-rippling of sufficiently short free graphene ribbons. Consequently, a critical length is estimated so that self-rippling occurs only when the length of free single-layer graphene ribbons is much longer than the critical length. The estimated critical length is reasonably consistent with the known fact that self-rippling cannot occur in shorter free graphene sheets (say, of length below 20 nm).

Finally, the effect of a rigid substrate on ripple formation is studied, and the results show that rippling can be suppressed and the graphene monolayer can be ultra-flat in the appearance of a rigid substrate due to the van der Waals interaction between the substrate and graphene. For varying distance between graphene and substrate, there exists a critical distance below which rippling in graphene monolayer cannot exist due to the strong van der Waals interaction. However, when the distance between substrate and graphene is at least few times larger than the critical distance. the effect of substrate can be ignored and the graphene monolayer can be treated approximately as a free-standing graphene monolayer.

Preface

Chapter 2, 3.1 and 3.2 of the thesis have been published as B. J. Wu, and C. Q. Ru. J. Appl. Phys., 120(2), 024304 (2016). I was responsible for math derivation, obtaining results and writing manuscript. Dr. C.Q. Ru was the supervisory author who proposed the topic, checked the results and revised the manuscript.

Chapter 3.3 of the thesis is expected to be submitted for publication soon. I am responsible for math derivation, obtaining results and writing manuscript. Dr. C.Q. Ru is the supervisory author who proposed the topic, checked the results and revised the manuscript.

Acknowledgements

I would like to gratefully thank my supervisor Dr. C.Q. Ru for his encouragement and support during my study. I also hope to say “thank you” to all fellow researchers in the Department of Mechanical Engineering at the University of Alberta and my family and friends who help and support me all the time.

Lastly, I want to thank the financial support from NSERC during my study.

Table of Contents

List of Figures

Chapter 1

Introduction

1.1 Literature review

Graphene is an atom-thick two-dimensional membrane of extraordinary thermal, mechanical, and electrical properties, with potential applications to nanotechnology. Its unique lattice honeycomb structure made it as a building block of other related materials, and it can be rolled to 1-D nanotube, stacked to 3-D graphite or wrapped to 0-D fullerenes. The in-plane strong σ-bonds between carbon atoms and long range π bonds perpendicular to the plane lead to lots of remarkable properties of graphene. For example, Mayorov et al. (2011) show that graphene on boron nitride at room temperature has the giant carrier mobility of $2\times10^5\ cm^{-2}V^{-1}S^{-1}$, Balandin (2011) reported that graphene had very high thermal conductivity (25 times that of silicon). Besides these, other properties such as a weak optical absorptivity of 2.3% (Nair et al, 2008), impermeability to any gases (Bunch et al, 2008), and ability to sustain densities a million times higher than that of copper (Moser et al. 2007) are also reported. Among the list of many extraordinary properties of graphene, its mechanical properties have aroused intense experimental and theoretical studies. For instance, Lee et al. (2008) investigated the Young's modulus and fracture strength of a monolayer graphene membrane by atomic force microscopy (AFM), reporting the values of 1 TPa and 130

GPa, respectively. For further details of elastic behavior of graphene membranes, see e.g. (Zhang et al, 2012) and cited references.

Single-layer graphene samples was first isolated from graphite by Geim et al (2004). This led to an explosion of interest, partly because perfect two-dimensional crystals cannot exist in the free state, according to the Mermin-Wagner theorem (Mermin, 1968). Long-wavelength fluctuations destroy the long-range order of 2D crystals, which means 2D membranes tends to be crumped in 3D space. However, these fluctuations can be suppressed by anharmonic coupling between bending and stretching mode meaning that a 2D membrane can exist but will exhibit strong height fluctuations (Fasolino et al. 2007) (see Fig. 1.1), which was called ripples. Such microscopic corrugations have a profound impact on electronic, chemical and mechanical properties of graphene sheets. For instance, conical singularities would be formed due to rippling (Pereira et al. 2010), which could markedly affect the conductivity and mobility of graphene. In addition, elasticity softening of graphene monolayer due to ripples was reported by Lee (2015). Therefore it is of great interest to understand the intrinsic driving force for self-rippling and to develop simple theoretical models for rippling-related mechanical phenomena.

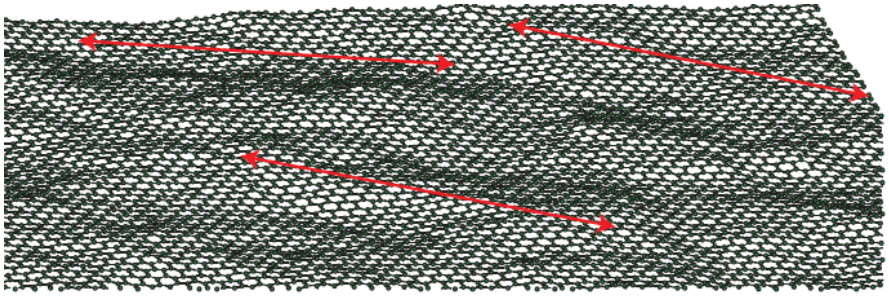

Fig.1.1 A representative configuration of a free single-layer graphene at room temperature (Fasolino et al. 2007-with the permission of the authors)

1.2 Motivation of the thesis

Various rippling mechanisms have been proposed, including thermal fluctuations (Fasolino et al. 2007, Gao et al. 2014), molecular absorption (Thompson-Flagg et al. 2009) or influence of grain boundaries (Capasso et al. 2014). In particular, it is believed that van der Waals attractive force plays a key role in rippling-related phenomena. For example, Zhu et al. (2012) found that van der Waals attractive force can cause narrow standing wrinkles. Based on an over-simplified geometrical shape of ripple mode, an approximate model was proposed in a previous work (Ru. 2013) for reduced van der Waals energy due to ripple formation. However, a technical difficulty associated with the simplified rippling energy expression is that the derived expression cannot be written as a desired smooth integral form of the deflection and its derivatives. This limits its applicability to other rippling-related mechanical phenomena. To overcome this limit, a deflection-based phenomenological integral expression for rippling energy

of graphene monolayer and its implications to rippling-related elastic behavior of graphene membranes will be examined in the present thesis.

1.3 The objectives and outline

The present work aims to develop a general phenomenological integral expression for rippling energy that drives ripple formation of free graphene sheets. In view of the fact that self-rippling of graphene monolayers is characterized by the out-of-plane deflection, we study all possible weakly-nonlinear, lower-order candidate integral expressions which have a somewhat similar mathematical form as the over-simplified model derived in (Ru. 2013). Under some reasonable restrictions, it is shown that a phenomenological expression can be selected uniquely with two undetermined coefficients which can be estimated by the observed wavelength and amplitude of associated ripple mode.

Specifically, the thesis includes:

1) In Chapter 2, all proposed candidate phenomenological integral expressions for the rippling energy are examined based on an admissibility criterion whether the candidate expression admits stable periodic ripple mode. The two coefficients for the admitted phenomenological integral expression are estimated based on the known values of the wavelength and amplitude of observed ripple mode. Besides these, In order to better understand the physical meaning of the two coefficients, the dependency of the two coefficients on wavelength for a few given specific values of the amplitude is given at the end of Chapter 2.

2) In Chapter 3, some application of the proposed model are discussed. First, the effect of an applied force on the ripple formation of single-layer graphene sheets is studied. Then, the effect of such a rippling energy on compressed buckling of a short graphene ribbon is discussed. Finally, based on the rippling energy expression, the effect of substrate on ripple formation is studied.

3) In Chapter 5, major conclusions are summarized and future work is recommended.

Chapter 2

A Phenomenological Expression for Rippling Energy of Free Graphene Monolayers

2.1 Admitted phenomenological expression for rippling energy of free graphene monolayers

2.1.1 Candidate expressions for rippling energy

In a previous paper (Ru, 2013), ripple formation of free single-layer graphene ribbons driven by the van der Waals-like rippling energy is studied based on a simplified geometrical model of a ripple mode. For such a simplified periodic ripple mode of amplitude A and wavelength λ (or the wavenumber m, where $\lambda = 2\pi / m$), the reduced rippling energy (per unit length) of a free single-layer graphene ribbon due to ripple formation was estimated as

$$-\beta m(A^2 m^2 - \alpha A^4 m^4), \tag{2.1}$$

where α and β are two positive coefficients, and an estimate of the coefficient β is given in (Ru, 2013). Since the rippling energy (2.1) is an odd function of the wavenumber m, it cannot be expressed into a desired smooth integral expression of the deflection and its derivatives. This limits the application of expression (2.1). Here, to overcome this shortcoming, we try to find an alternative even-order expression which is qualitatively similar to (1) but can be written as a smooth integral form.

We study all possible phenomenological expressions which have a similar mathematical form as (2.1) but are even-order in both the wavenumber m and the amplitude A and thus are invariant with respect to the change in the sign of the deflection $w(x)$ and the positive direction of x-axis. Here, we shall confine ourselves to the weakly nonlinear and lower-order cases when the (nonlinear) governing differential equation for the deflection is not higher than sixth-order. For a periodic ripple mode $w(x) = A\sin(mx)$, all such possible two-term, weakly-nonlinear and lower-order integral expressions for rippling energy are list as below

$$-\mu A^2 m^2 (1-\gamma A^2 m^{2N}), \mu > 0, \gamma > 0, N \geq 0, \tag{2.2}$$

$$-\mu_1 (A^2 m^6 - \gamma_1 A^4 m^{2N_1}), \mu_1 > 0, \gamma_1 > 0, N_1 \geq 0, \tag{2.3}$$

$$-\mu_2 (A^4 m^2 - \gamma_2 A^4 m^{2N_2}); \mu_2 > 0, \gamma_2 > 0, N_2 \geq 2, \tag{2.4}$$

$$-\mu_3 (A^4 m^4 - \gamma_3 A^4 m^{2N_3}); \mu_3 > 0, \gamma_3 > 0, N_3 \geq 3, \tag{2.5}$$

where N and N_i (i=1,2,3) are some non-negative integers, and the parameter pair μ and γ (or μ_i and $\gamma_i, i = 1,2,3$) are two positive parameters, to be determined by experimental data of the wavelength and amplitude of observed ripple mode. Here the second term of expressions (2.2-2.5) is higher-order than the first term either in the amplitude A or in the wavenumber m, thus we set $N_2 \geq 2$ for (4) and $N_3 \geq 3$ for (5). The expressions (2.2-2.5) are a complete list of all possible such two-term, weakly-nonlinear, lower-order integral expressions. Among these candidate expressions, we shall select the right one which admits stable periodic ripple mode.

2.1.2 An admitted expression for rippling energy

Since the form (2.2) has been confirmed (Ru, 2013) to admit stable ripple mode (when and only when $N = 0$), the admissibility of the other three candidate expressions (2.3-2.5) is examined based on a criterion whether it admits stable periodic ripple mode.

Rejection of candidate form (2.3)

With the candidate form (2.3) and bending strain energy, the total potential energy (per unit length) of a free single-layer graphene ribbon for a periodic ripple mode $w(x) = A\sin(mx)$ is

$$U_1(A,m) = \frac{EI}{2}A^2m^4(1+\frac{1}{4}A^2m^2) - \mu_1(A^2m^6 - \gamma_1 A^4 m^{2N_1}), \mu_1 > 0, \gamma_1 > 0, N_1 \geq 0, \tag{2.6}$$

where EI is the bending rigidity of the ribbon. Minimizing of the energy form (2.6) with respect to A^2 and m^2 gives two conditions

$$\begin{cases} \frac{EI}{2}(1+\frac{1}{2}A^2m^2) - \mu_1 m^2 + 2\gamma_1\mu_1 A^2 m^{2N_1-4} = 0, \\ \frac{EI}{2}(2+\frac{3}{4}A^2m^2) - 3\mu_1 m^2 + N_1\gamma_1\mu_1 A^2 m^{2N_1-4} = 0. \end{cases} \tag{2.7}$$

Eliminating $\mu_1 m^2$ from equation (2.7) gives an equation:

$$\frac{EI}{2}(1+\frac{3}{4}A^2m^2) = (N_1-6)\gamma_1\mu_1 A^2 m^{2N_1-4}. \tag{2.8}$$

Since LHS of (2.8) is positive, expression (2.6) doesn't admit stable ripple mode when $N_1 < 7$. Thus, because we shall confine ourselves to the lower-order case when the governing differential equation for the deflection is not higher than fourth-order, the number N_1 for (2.3) is not larger than 6, as mentioned previously. Therefore the candidate form (2.3) doesn't admit stable ripple mode and thus is rejected.

Rejection of candidate form (2.4)

With the rippling energy form (2.4), the total potential energy (per unit length) of a free single-layer graphene ribbon for a periodic ripple mode $w(x) = A\sin(mx)$ is

$$U_2(A,m) = \frac{EI}{2}A^2m^4(1+\frac{1}{4}A^2m^2) - \mu_2(A^4m^2 - \gamma_2 A^4 m^{2N_2}); \mu_2 > 0, \gamma_2 > 0, N_2 \geq 2. \tag{2.9}$$

Minimizing of the energy (2.9) gives two conditions,

$$\begin{cases} \frac{EI}{2}(1+\frac{1}{2}A^2m^2) - 2\mu_2\frac{A^2}{m^2} + 2\gamma_2\mu_2 A^2 m^{2N_2-4} = 0, \\ \frac{EI}{2}(2+\frac{3}{4}A^2m^2) - \mu_2\frac{A^2}{m^2} + N_2\gamma_2\mu_2 A^2 m^{2N_2-4} = 0. \end{cases} \tag{2.10}$$

Eliminating $\mu_2\frac{A^2}{m^2}$ from equation (2.10) gives an equation

$$\frac{EI}{2}(3+A^2m^2) = (2-2N_2)\gamma_2\mu_2 A^2 m^{2N_2-4}. \tag{2.11}$$

Since LHS of (2.11) is positive, N_2 must be zero. Thus the candidate form (2.4) is rejected too.

Rejection of candidate form (2.5)

With the bending strain energy and the candidate rippling energy (2.5), the total potential energy (per unit length) of a free single-layer graphene ribbon for a periodic ripple mode $w(x) = A\sin(mx)$ is

$$U_3(A,m)=\frac{EI}{2}A^2m^4(1+\frac{1}{4}A^2m^2)-\mu_3(A^4m^4-\gamma_3A^4m^{2N_3});\mu_3>0,\gamma_3>0,N_3\geq 3 \tag{2.12}$$

Minimizing of the energy (2.12) gives two conditions,

$$\begin{cases}\frac{EI}{2}(1+\frac{1}{2}A^2m^2)-2\mu_3A^2+2\gamma_3\mu_3A^2m^{2N_3-4}=0\\ \frac{EI}{2}(2+\frac{3}{4}A^2m^2)-2\mu_3A^2+N_3\gamma_3\mu_3A^2m^{2N_3-4}=0\end{cases} \tag{2.13}$$

Eliminating μ_3A^2 from equation (2.13) gives an equation:

$$\frac{EI}{2}(1+\frac{1}{4}A^2m^2)=(2-N_3)\gamma_3\mu_3A^2m^{2N_3-4} \tag{2.14}$$

Since LHS of (2.14) is positive, N_3 must be smaller than 2. Thus the candidate form (2.5) is rejected too.

In summary, it is concluded that, among all four candidate forms (2.2-2.5), only the form (2.2) admits stable periodic mode, while all other 3 candidate forms (2.3-2.5) are rejected because none of them admits stable periodic ripple mode. For a free-standing graphene ribbon treated as an elastic beam, if the rippling energy has the form (2.2), the total potential energy can be written into a desired elegant integral form as

$$U_L(A,m)=\frac{EI}{2}\int_0^L(w_{xx})^2[1+(w_x)^2]dx-\mu\int_0^L(w_x)^2(1-4\gamma w^2)dx, \tag{2.15}$$

where L is the length of the graphene ribbon. For a periodic ripple mode $w(x)=A\sin(mx)$, the total potential energy (per unit length) of the graphene ribbon is

$$U(A,m)=\frac{EI}{2}A^2m^4(1+\frac{1}{4}A^2m^2)-\mu A^2m^2(1-\gamma A^2). \tag{2.16}$$

Obviously the rippling energy of (2.16) is identical to the admitted form (2.2) with N=0. It is seen from (2.15) that the selected rippling energy (2.2) contains two terms: one quadratic term which has a destabilizing effect and acts like a compressive force (2μ), and the other fourth-order term which has a stabilizing effect and acts like a nonlinear elastic foundation. It is their nonlinear combined effect that selects a finite wavelength of the stable ripple mode for a sufficiently long free graphene ribbon, which is much smaller than the length of the ribbon. It should be mentioned that the present thesis focuses on periodic ripples and use them to identify the two coefficients of the proposed model. Once the proposed model is well identified, it could be used to study other mechanical phenomena such as randomly distributed non-periodic ripples. In what follows, we will focus on the selected integral form (2.15) and its explicit expression (2.16) for a periodic ripple mode $w(x) = A\sin(mx)$.

2.2 Estimation of the two coefficients (γ, μ)

With the selected integral form (2.15) and the associated total energy (2.16) for a periodic ripple mode $w(x) = A\sin(mx)$, the minimization conditions give

$$\begin{cases} \dfrac{EI}{2}(m^2 + \dfrac{1}{2}A^2m^4) - \mu + 2\gamma\mu A^2 = 0, & (2.17a) \\ \dfrac{EI}{2}(2m^2 + \dfrac{3}{4}A^2m^4) - \mu + \gamma\mu A^2 = 0. & (2.17b) \end{cases}$$

It follows from Eqs. (2.17a) and (2.17b) that

$$\begin{cases} \mu = \dfrac{EI}{2}(3 + A^2 m^2) m^2, \\ \gamma = \dfrac{1}{A^2} \dfrac{1 + \dfrac{1}{4} A^2 m^2}{3 + A^2 m^2}, \end{cases} \tag{2.18}$$

where EI is the bending rigidity of graphene ribbons. For example, because the bending rigidity (per unit width) of single-layer graphene sheets is about 1 eV (Lindahl et al. 2012). A single-layer graphene ribbon of width b has $EI = b \times 1eV$. Since EI is proportional to the width b of graphene ribbon, the parameter μ given by (2.18) is proportional to the width while γ is independent of the width. Here, we determine the parameter pair μ, γ for a graphene ribbon of width b based on known experimental data of the wavelength and amplitude of observed ripple mode.

There exist extensive experimental data on wavelength and amplitude of ripple modes of monolayer graphene, which widely vary with boundary support, substrate or thermal stress. Here we focus on free-standing monolayer graphene at room temperature without any boundary support, substrate or thermal stress. With transmission electron microscopy (TEM), Meyer et al. (2007) measured the wavelength of $\approx 10nm$ and amplitude of $\approx 1nm$. Bangert et al. (2009) used aberration-corrected scanning transmission electron microscope (superSTEM) to study ripples of free-standing monolayer graphene, and the wavelength and amplitude were estimated to be $\approx 10nm$ and $\approx 0.5nm$, respectively. Zan et al. (2012) found that ripples in free-standing monolayer graphene have wavelengths of 5 to 10 nm, and amplitudes of typically 0.5nm. In addition, Breitwieser et al. (2014) reported ripple formation of free-standing single-

layer graphene with wavelength of $\approx 6nm$ and amplitude of $\approx 1nm$. Thus the estimated ranges of the two coefficients γ and μ by (2.18) are

$$\begin{cases} \dfrac{\mu}{b} \approx 0.107 : \ 0.427(Jm^{-2}), \\ \gamma \approx 3.3\times 10^{17} \ : \ 1.3\times 10^{18}(m^{-2}), \end{cases} \tag{2.19}$$

which give the wavelength ranging from 5 nm to 10 nm and the amplitude ranging from 0.5 nm to 1 nm at room temperature. As temperature changes, it is known that free graphene ribbons exhibit a negative coefficient of thermal expansion mainly due to rippling-induced contraction (Mounet et al. 2005, Yoon et al. 2011). For a periodic ripple mode $w(x) = A\sin(mx)$, since rippling does not cause stretching strain of free graphene, the effective contraction of graphene ribbons given by the present model is (Khamlichi, 2001)

$$\Delta L = \int (\sqrt{1-[\frac{2\pi}{\lambda} A\cos(\frac{2\pi}{\lambda} x)]^2} - 1)dx. \tag{2.20}$$

For weakly nonlinear deflections, the average contraction strain ε is given by

$$\varepsilon = \frac{\Delta L}{L} \approx -(\pi A / \lambda)^2. \tag{2.21}$$

If the weak temperature-dependence of other parameters (such as the negative coefficient of thermal expansion of graphene) is neglected, it follows from (2.21) that the change of the squared ratio $(\frac{A}{\lambda})^2$ is directly proportional to the change of temperature, qualitatively consistent with existing literature (Fasolino, 2007).

2.3 Discussion on the two coefficients (μ, γ)

In order to better understand the physical meaning of the two parameters μ and γ, the dependency of the two parameters on wavelength for a few given specific values of the amplitude A is given in Figs. 1 and 2.

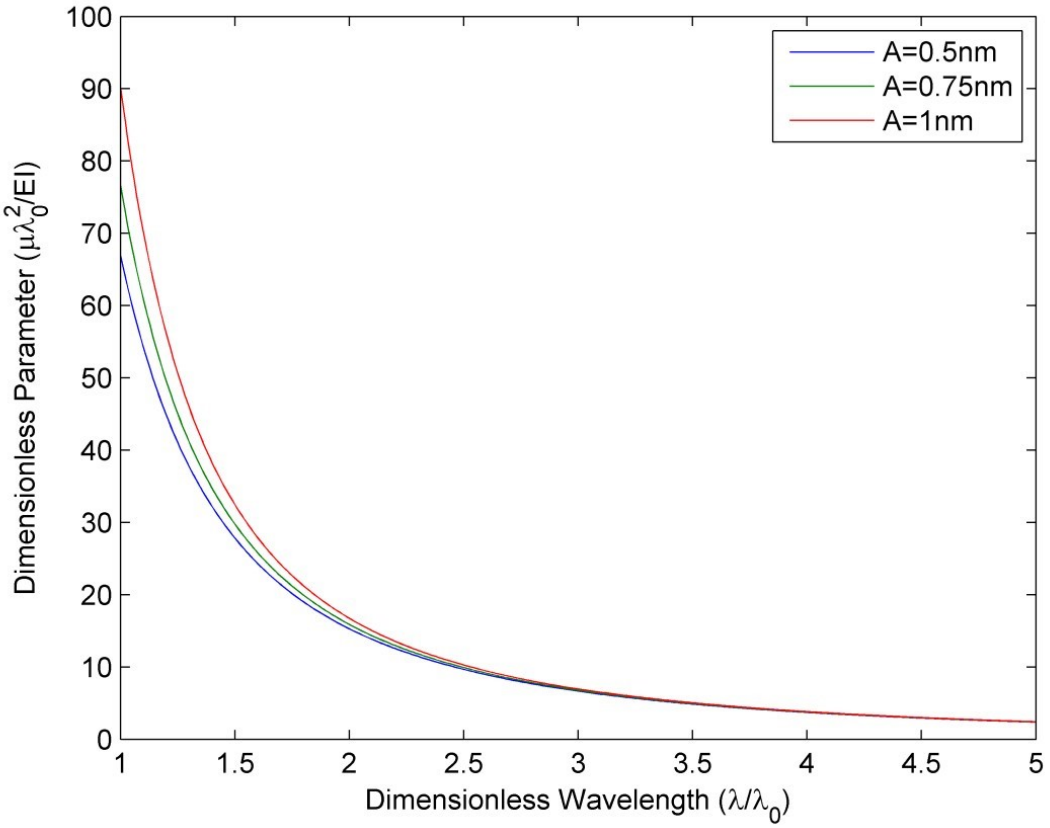

Fig. 2.1 The dependence of the parameter $\mu\lambda_0^2 / EI$ on the wavelength λ / λ_0 ($\lambda_0 = 5nm$)

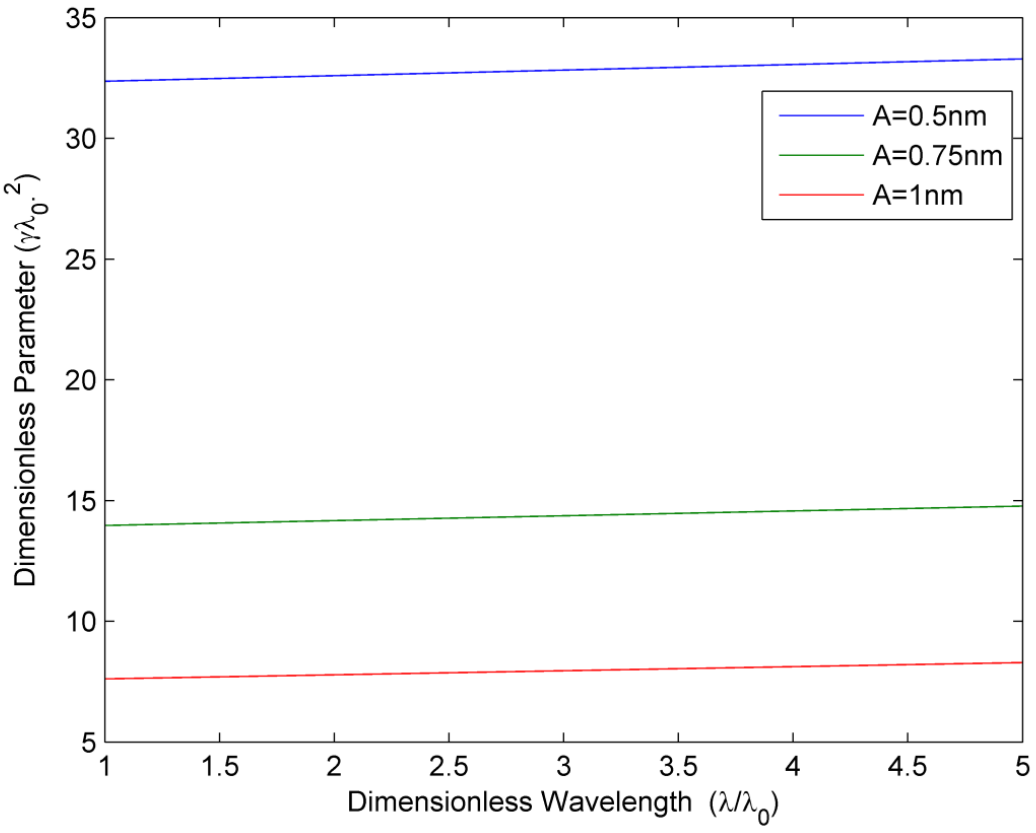

Fig. 2.2 The dependence of the parameter $\gamma\lambda_0^2$ on the wavelength λ / λ_0 ($\lambda_0 = 5nm$)

It can be seen from Fig. 2.1 and Fig. 2.2 that the coefficient μ of the quadratic term (which acts like a compressive force) decreases with the wavelength but is insensitive to the amplitude. On the other hand, the coefficient γ of the fourth-order term (which acts like a nonlinear elastic foundation) decreases with the amplitude but is insensitive to the wavelength. Actually, because the data for single-layer graphene sheets meet the condition $A^2m^2 = 3$, thus Eq. (2.19) can be simplified to the following approximate form

$$\begin{cases} \mu \approx \dfrac{3EI}{2} m^2, \\ \gamma \approx \dfrac{1}{3A^2}. \end{cases} \tag{2.22}$$

It is seen from Eq. (2.22) that when the thickness of an elastic ribbon increases, because EI increases with cube of thickness (such as a continuum thin beam or a thick multilayer graphene sheets without interlayer sliding) but the coefficient μ of self-rippling energy scales with thickness, the wavelength (determined by the wavenumber m by $\lambda = 2\pi / m$) will increase quickly with increasing thickness. This implies that small-wavelength ripple modes are unlikely for relatively thick ribbons if interlayer sliding is prohibited, which is roughly consistent with experimental observation of multilayer graphene sheets (Wang et al, 2012). Indeed, the present model predicts that the extremely low bending rigidity of atom-thick monolayers, such as single-layer graphene sheets, is essentially responsible for observed stable periodic ripple mode. On the other hand, self-rippling is unlikely for thicker ribbons such as continuum elastic thin beams even only a few nanometers in thickness.

2.4 Conclusions

In summary, it can be concluded:

1) Based on a criterion whether the model admits stable periodic ripple mode, an integral form along with two undetermined coefficients is selected uniquely among all possible two-term, weakly-nonlinear and lower-order integral expressions for rippling energy.

2) The two coefficients for the admitted phenomenological integral expression can be well estimated based on the known values of the wavelength and amplitude of observed ripple mode.

3) One of two associated coefficients of the proposed expression is largely determined by the wavelength but insensitive to the amplitude of ripple mode, while the other one is essentially determined by the amplitude but insensitive to the wavelength

Chapter 3

Some Application of the Proposed Model

3.1 The effect of an applied force on ripple formation

3.1.1 Formulation

It is of great interest to study the effect of an applied force on ripple formation. With a total resultant axial force T (tensile or compressive) applied to an elastic beam, the potential energy of the elastic beam of length L is given by (Khamlichi, 2001)

$$\frac{EI}{2}\int_0^L (w_{xx})^2[1+(w_x)^2]dx+\frac{T}{2}\int_0^L (w_x)^2[1+\frac{1}{4}(w_x)^2]dx. \qquad (3.1)$$

In which, $T>0$ stands for tensile force and $T<0$ stands for compressive force.

Thus, for a periodic rippling mode $w(x)=A\sin(mx)$ and with the rippling energy (2.2), the total potential energy (per unit length) of a single-layer graphene ribbon subjected to a constant axial force T is

$$U_{total}(A,m)=\frac{EI}{2}A^2m^4(1+\frac{1}{4}A^2m^2)+\frac{T}{2}A^2m^2\times(1+\frac{3}{16}A^2m^2)-\mu A^2m^2(1-\gamma A^2). \qquad (3.2)$$

Minimizing Eq. (3.2) with respect to both A^2 and m^2 gives two conditions:

$$\begin{cases} \frac{EI}{2}(3m^2 + A^2m^4) + \frac{T}{2}(1 + \frac{3}{8}A^2m^2) - \mu = 0, & (3.3a) \\ \frac{EI}{2}(m^2 + \frac{1}{4}A^2m^4) - \gamma\mu A^2 = 0. & (3.3b) \end{cases}$$

As we discussed before, it is seen from Eq. (2.21) that contraction of graphene ribbon becomes significant particularly for short-wavelength rippling under high compressive force. Thus actual deformed wavelength is given by $\lambda' = (1+\varepsilon)\lambda$, where λ is the wavelength in the undeformed configuration.

3.1.2 Results and comparison with known data

The effect of an applied force (T/μ) on the deformed wavelength (which is the wavelength observed in experiments) and the associated amplitude-wavelength ratio of the ripple mode is shown in Fig. 3.1 for a graphene nanoribbon of width b with a chosen typical parameter pair $\mu/b = 0.427(Jm^{-2}), \gamma = 1.3\times10^{18}(m^{-2})$.

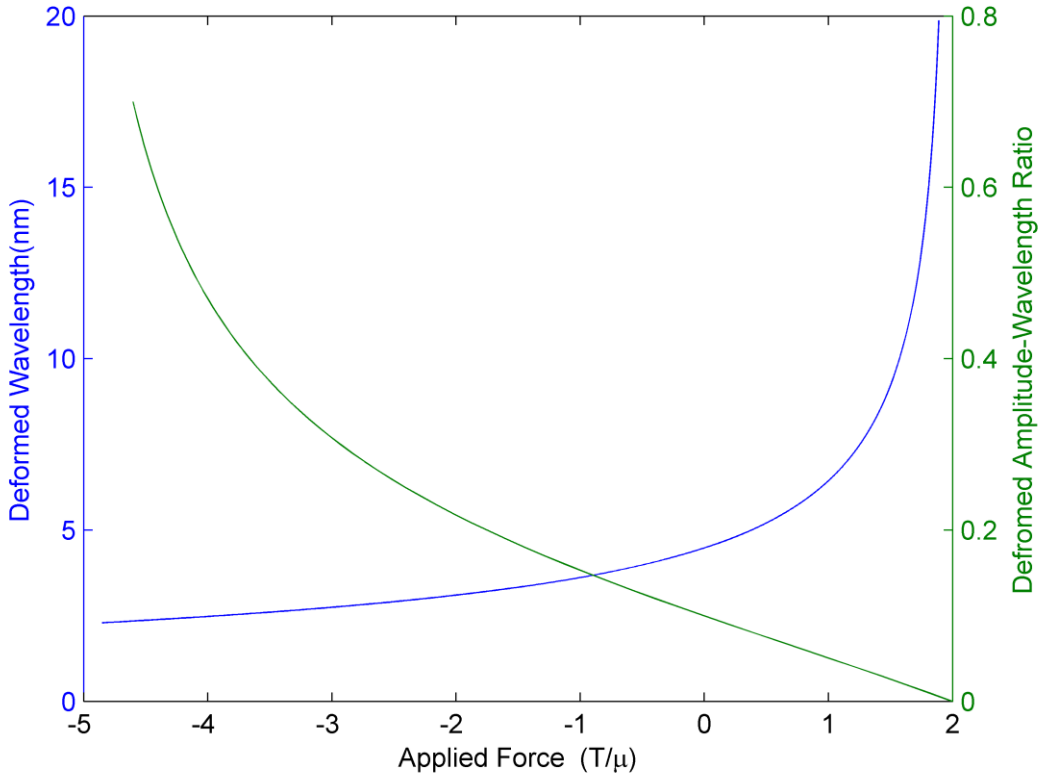

Fig. 3.1 The effect of an applied force (T/μ) on "deformed wavelength" and "deformed amplitude-wavelength ratio"

Fig. 3.1 indicates that there exists a maximum tensile force (2μ) and a maximum compressive force (-5μ), beyond which the stable periodic ripples cannot exist. Indeed, it follows from Eq. (3.3a) that

$$T = 2 \times \frac{\mu - \frac{EI}{2}(3m^2 + A^2 m^4)}{(1 + \frac{3}{8} A^2 m^2)}. \tag{3.4}$$

Thus, there is not a periodic rippling mode $w(x) = A\sin(mx)$ for any tensile force $T > 2\mu$. Actually, it is readily seen from (3.4) that for any tensile force $T > 2\mu$, positive amplitude A cannot exist. Therefore we define $T_{cr} = 2\mu$ as the minimum tensile force to suppress ripples. On the other hand, for any $T < T_{cr}$ (no matter tensile or compressive), it can be verified that the mode given by Eqs. (3.3a) and (3.3b) satisfies the stability conditions

$$\begin{aligned}
&\frac{\partial^2 U(A,m)}{\partial(A^2m^2)^2} = \frac{EI}{2}\left(\frac{5A^2m^2+16}{8A^2+3A^4m^2}\right) + \frac{3\mu}{8+3A^2m^2} > 0;\\
&\frac{\partial^2 U(A,m)}{\partial(m^2)^2} = \frac{2\gamma\mu A^4}{m^2} > 0;\\
&\begin{vmatrix} \dfrac{\partial^2 U(A,m)}{\partial(A^2m^2)^2} & \dfrac{\partial^2 U(A,m)}{\partial(A^2m^2)\partial(m^2)} \\ \dfrac{\partial^2 U(A,m)}{\partial(A^2m^2)\partial(m^2)} & \dfrac{\partial^2 U(A,m)}{\partial(m^2)^2} \end{vmatrix} = \frac{E^2I^2}{4}\left(\frac{48+30A^2m^2+5A^4m^4}{16+6A^2m^2}\right)\\
&+\frac{3EI\mu(2+\frac{1}{2}A^2m^2)A^2}{16+6A^2m^2} > 0.
\end{aligned} \tag{3.5}$$

It is noticed that Eq. (3.3b) is no longer valid if the rippling energy is absent (μ=0, γ=0), which implies that the rippling energy is essential for the existence of stable periodic ripples.

On the other hand, it follows from Eq. (3.3b) that

$$A^2 = \frac{\frac{EI}{2}m^2}{\gamma\mu - \frac{EI}{8}m^4}. \tag{3.6}$$

Therefore, we have the restriction

$$\lambda^4 > \frac{2\pi^4 EI}{\gamma\mu}. \tag{3.7}$$

Thus, there exists a minimum wavelength $\lambda_{\min} = (\frac{2\pi^4 EI}{\gamma\mu})^{1/4}$ and the associated minimum deformed wavelength $\lambda'_{\min} = (1+\varepsilon)\lambda_{\min}$, below which stable periodic ripples will not exist. The predicted minimum deformed wavelength is about 2.2 nm, reasonably consistent with some observed minimum wavelength 2 nm (Bai et al. 2014), and the associated maximum compressive force (per unit width) is about -2.1 nN/nm beyond which stable periodic ripple modes will not exist. This is consistent with the fact that ripples would be collapsed into narrow standing wrinkles with large amplitude-to-wavelength ratio (Zhang & Arroyo, 2014) under sufficient compressive stress.

The present model predicts that the wavelength will increase with an applied tensile force and there exists a minimum tensile force to suppress ripples. This is consistent with the fact that ripples can be controlled (Bai et al, 2014) or even fully suppressed (Lui et al, 2009. Xue et al. 2011) with an applied tensile force (say, induced by a substrate). The minimum tensile force (per unit width) to suppress ripples, given by the present model with $T_{cr} = 2\mu$ and (2.19) is about $(214-854)\,pN/nm$ when the wavelength of free rippling mode varies from 5 nm to 10 nm. Using in plane elastic modulus $E_{2D} \approx 340N/m$ (Lee et al. 2009) and the nominal thickness 0.34nm of single-layer graphene, the corresponding tensile strain given by the present model is about $0.06\% : 0.26\%$. In particular, if the wavelength of free rippling mode is around 6 nm, the minimum tensile strain given by the present model is about 0.16%, in remarkable

agreement with known related data 0.25% (Roldán et al, 2011) where the wavenumber of free rippling is around 1/nm (which corresponds to a wavelength of $\approx 6nm$). Actually, it has been a real challenge for us to find more available data on the minimum tensile strain to suppress ripples. Here, we would mention that some recent experiment on strained graphene showed that in plane effective elastic modulus could increase to : $700N/m$ under a pre-strains above 0.5% (Polin et al, 2015). It remains unclear whether this interesting phenomenon could be partially attributed to ripples under a pre-strain.

3.1.3 Conclusions

In summary, it can be concluded:

1) With an applied tensile force, ripples can be controlled or even fully suppressed. This conclusion is consistent with relative references, such as (Lui et al, 2009).

2) The minimum tensile strain to eliminate rippling is determined by the coefficient μ, and is about 0.06%-0.26% when μ varies within the range given by (2.19). In particular, if the wavelength of free rippling mode is around 6 nm, the minimum tensile strain given by the present model is about 0.16%, in remarkable agreement with known related data 0.25% (Roldán et al, 2011) where the wavenumber of free rippling is around 1/nm (which corresponds to a wavelength of $\approx 6nm$).

3) Under a sufficient compressive stress, the present model predicts that ripples would be collapsed into narrow standing wrinkles of minimum wavelengths around 2.2 nm, reasonably consistent with some observed minimum wavelength 2 nm (Bai et al. 2014).

3.2 Compressed buckling of a short graphene ribbon of limited length

As mentioned previously, the selected rippling energy (2.2) contains two terms: a destabilizing quadratic term which acts like a compressive force (2μ), and a stabilizing higher-order term which acts like a nonlinear elastic foundation. It is their nonlinear combined effect that selects a finite wavelength for ripple mode which is usually much smaller than the length of free-standing graphene ribbon. All of previous analysis is based on an assumption that the wavelength of ripple mode is much smaller than the length of graphene ribbon and thus the constraint conditions at the two ends of the ribbon are negligible. Now let us consider buckling of a singlelayer graphene ribbon of limited finite length L under a constant compressive force P. In this case, the applied compressive force P is needed for compressed buckling with traditional buckling mode because the rippling energy characterized by the two parameters (γ, μ) is relatively weak and cannot drive self-rippling of a sufficiently short graphene ribbon.

3.2.1 Governing equation and boundary conditions

First, let us derive basic governing equation for a compressed graphene ribbon in the presence of the rippling energy defined by (2.2). In this case, the total potential energy of the ribbon under a constant compressive force P is given by

$$V = \frac{EI}{2}\int_0^L (w_{xx})^2[1+(w_x)^2]dx - \frac{P}{2}\int_0^L (w_x)^2[1+\frac{1}{4}(w_x)^2]dx \\ -\mu\int_0^L (w_x)^2(1-4\gamma w^2)dx. \tag{3.8}$$

Let

$$V_1 = \frac{EI}{2}\int_0^L (w_{xx})^2[1+(w_x)^2]dx,$$
$$V_2 = -\frac{p}{2}\int_0^L (w_x)^2[1+\frac{1}{4}(w_x)^2]dx, \tag{3.9}$$
$$V_3 = -\mu\int_0^L (w_x)^2(1-4\gamma w^2)dx,$$

we have

$$\delta V_1 = EI\int_0^L (w_{xxxx}[1+(w_x)^2]+4w_x w_{xx}w_{xxx}+(w_{xx})^3)(\delta w)dx$$
$$+EIw_{xx}[1+(w_x)^2](\delta w)_x\Big|_0^L - EI(w_{xxx}[1+(w_x)^2]+w_x(w_{xx})^2)\delta w\Big|_0^L, \tag{3.10}$$

$$\delta V_2 = -\frac{P}{2}\int_0^L [2w_x+(w_x)^3]d(\delta w)$$
$$= -\frac{P}{2}[2w_x+(w_x)^3]\delta w\Big|_0^L + \frac{P}{2}\int_0^L [2w_{xx}+3(w_x)^2 w_{xx}](\delta w)dx, \tag{3.11}$$

$$\delta V_3 = \int_0^L [2\mu w_{xx}(1-4\gamma w^2)-8\mu\gamma w(w_x)^2](\delta w)dx$$
$$-2\mu w_x(1-4\gamma w^2)(\delta w)\Big|_0^L \quad . \tag{3.12}$$

Combining (3.10), (3.11) and (3.12) gives δV

$$\delta V = \int_0^L (EIw_{xxxx}[1+(w_x)^2]+4EIw_x w_{xx}w_{xxx}+EI(w_{xx})^3+Pw_{xx}+\frac{3}{2}P(w_x)^2 w_{xx}+$$
$$2\mu w_{xx}(1-4\gamma w^2)-8\mu\gamma w(w_x)^2)(\delta w)dx+EIw_{xx}[1+(w_x)^2](\delta w)_x\Big|_0^L - \tag{3.13}$$
$$\{EIw_{xxx}[1+(w_x)^2]+EIw_x(w_{xx})^2+\frac{P}{2}[2w_x+(w_x)^3]+2\mu w_x(1-4\gamma w^2)\}\delta w\Big|_0^L = 0.$$

Since δw is arbitrary in the graphene ribbon, the governing equation is given by

$$EI\frac{d^4w}{dx^4}+EI\frac{d^4w}{dx^4}(\frac{dw}{dx})^2+4EI\frac{dw}{dx}\frac{d^2w}{dx^2}\frac{d^3w}{dx^3}+EI(\frac{d^2w}{dx^2})^3+P\frac{d^2w}{dx^2}$$
$$+\frac{3}{2}P(\frac{dw}{dx})^2\frac{d^2w}{dx^2}+2\mu\frac{d^2w}{dx^2}-8\mu\gamma\frac{d^2w}{dx^2}w^2-8\mu\gamma w(\frac{dw}{dx})^2=0. \tag{3.14}$$

In the absence of the rippling energy (2.2), for example, equation (3.14) agrees with the weakly nonlinear equation (2) of (Hunt et al. 1993). The derived weakly-nonlinear equation (3.14) could be used to study other rippling-related large deflection behavior of graphene ribbons in the presence of rippling energy.

On the other hand, the boundary conditions given by (3.13) are

$$\begin{aligned} &EIw_{xxx}[1+(w_x)^2]+EIw_x(w_{xx})^2+\frac{P}{2}[2w_x+(w_x)^3] \\ &+2\mu w_x(1-4\gamma w^2)=0 \quad or \quad \delta w=0, \\ &EIw_{xx}[1+(w_x)^2]=0 \quad or \quad (\delta w)_x=0, \end{aligned} \tag{3.15}$$

which give the following 3 types of boundary conditions

$$fixed: w=0, w_x=0; \tag{3.16a}$$
$$hinged: w=0,\ w_{xx}=0; \tag{3.16b}$$
$$free: w_{xx}=0, EIw_{xxx}[1+(w_x)^2]+\frac{P}{2}[2w_x+(w_x)^3]+2\mu w_x(1-4\gamma w^2)=0. \tag{3.16c}$$

3.2.2 Linear buckling analysis and critical length L_{cr}

To validate the proposed model, let us ignore all nonlinear terms of equation (3.14), it turns into

$$EI\frac{d^4w}{dx^4}+P\frac{d^2w}{dx^2}+2\mu\frac{d^2w}{dx^2}=0. \tag{3.17}$$

Since now we consider a graphene ribbon of finite length, the role of boundary condition cannot be neglected. First let us suppose that the buckling mode for a hinged graphene ribbon which satisfies the boundary conditions (3.16b) at both ends as

$$w = B\sin(\frac{n\pi}{L}x), n = 1,2,3... \tag{3.18}$$

Substituting Eq. (3.18) into Eq. (3.17), the lowest critical load can be obtained by $n = 1$

$$P_{cr} = \frac{EI\pi^2}{L^2} - 2\mu. \tag{3.19}$$

For sufficiently long graphene ribbons, the first term on RHS of Eq. (3.19) (which is the critical compressive force in the absence of the rippling energy) can be extremely low and ignorable as compared to the second term (2μ), and thus the rippling energy dominates and determines the nonlinear ripple mode of small wavelength (rather than the classical linear bucking mode (3.18)). For sufficiently short graphene ribbons, however, the first term on (3.18) becomes dominant over the second term and thus an applied compressive force $P_{cr} > 0$ is needed for compressed buckling of the short ribbon with the classical linear bucking mode (3.18). Therefore, for given value of μ, a critical length L_{cr} can be determined by setting $P_{cr} = 0$ in (3.18). In particular, the defined critical length of graphene ribbons is independent of their width.

The predicted critical length changes between 1.5-3 nm with the range of μ given in Eq. (2.19). Similarly, if we choose the buckling mode $w = B(1-\cos(\frac{2n\pi}{L}x)), n = 1,2,3...$

which satisfies the boundary conditions (3.16a) for a doubly-clamped graphene ribbon, the estimated critical length is from 3-6 nm. When the length of graphene ribbon is much larger than L_{cr}, the rippling energy is dominant and strong enough to drive self-rippling with nonlinear periodic mode of small wavelength. On the other hand, when the length of graphene ribbon is comparable or smaller than L_{cr}, the rippling energy cannot drive self-rippling, and an additional compressive force is needed for traditional compressed buckling of the short ribbon with the classical linear bucking mode. This result is consistent with related reference (Carlsson et al, 2007) where it was reported that small-sized graphene membranes do not show self-rippling, whereas macroscopic membranes have significant ripples. Moreover, the above estimated critical lengths (a few nanometers), are reasonably consistent with some known references (Thompson-Flagg et al, 2009) where the authors reported a flat monolayer graphene sample of size $10nm \times 10nm$ and (Fasolino et al, 2007) and only graphene samples of length larger than 20 nm could show significant self-rippling.

3.2.3 Initial post-buckling of a short graphene ribbon.

For sufficiently short graphene ribbons, self-rippling with multi-wave mode is unlikely and the classical buckling mode dominates. In this case, let us examine initial post-buckling of a short graphene ribbon driven by the rippling energy with no external force ($P = 0$). For example, for a short hinged graphene ribbon, substituting the linear buckling mode $w = B\sin(\frac{\pi}{L}x)$ into Eq. (3.14), the potential energy as a function of amplitude B is given by

$$V(B)=\frac{EIB^2\pi^4}{4L^3}+\frac{EIB^4\pi^6}{16L^5}-\frac{\mu B^2\pi^2}{2L}+\frac{\gamma\mu B^4\pi^2}{2L}. \tag{3.20}$$

The equilibrium of post-buckling is determined by $\frac{dV(B)}{dB}=0$, which gives

$$B\times[(EI\pi^4+8\gamma\mu L^4)B^2-4\mu L^4+4\mu L^2L_{cr}^2]=0. \tag{3.21}$$

Clearly, it can be seen from Eq. (3.21) that $B=0$ is the only solution for any $L\le\sqrt{\frac{EI\pi^2}{2\mu}}=L_{cr}$. However, when $L>L_{cr}$, a positive amplitude can be determined by the following expression

$$B^2=\frac{4\mu L^4-4\mu L^2L_{cr}^2}{EI\pi^4+8\gamma\mu L^4}. \tag{3.22}$$

Similarly, for a short clamped graphene ribbon, when $L>\sqrt{\frac{2EI\pi^2}{\mu}}=L_{cr}$, the amplitude can be determined as below

$$B^2=\frac{2\mu L^4-2\mu L^2L_{cr}^2}{8EI\pi^4+20\gamma\mu L^4}. \tag{3.23}$$

To study the effect of rippling energy on small-amplitude initial post-buckling ($B/L=1$) of a short graphene ribbon, the relation between the amplitude and various length $L>L_{cr}$ for different given boundary condition is shown in Fig. 3.2.

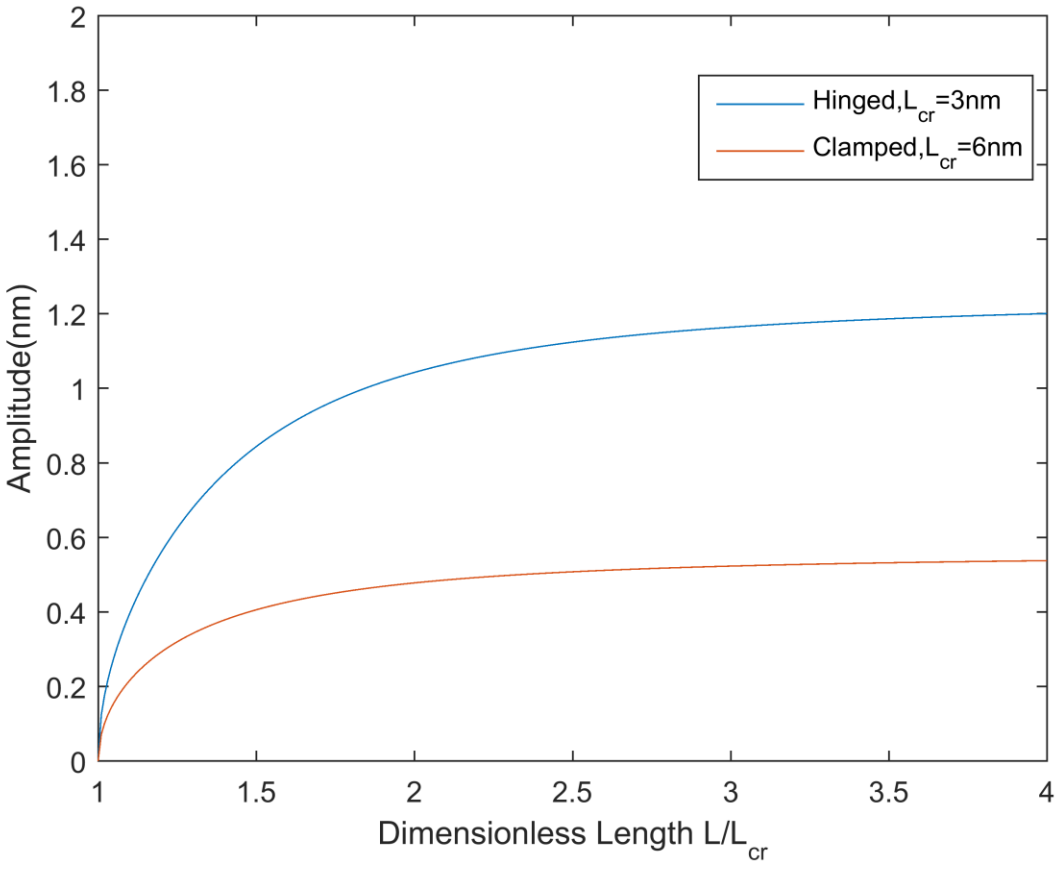

Fig. 3.2 The amplitude B as a function of different length of short graphene ribbon for different boundary conditions ($\mu / b = 0.107(Jm^{-2}), \gamma = 3.3\times10^{17}(m^{-2})$)

It is seen from Fig. 3.2 that for both clamped and hinged boundary conditions, the amplitude of buckling mode driven by the rippling energy is insensitive to the length when the graphene ribbon has a length more than 1.5-2 times the critical length L_{cr}, and the amplitude depends on boundary constrains, which means that boundary effect cannot be ignorable for the buckling behavior of short graphene ribbons.

3.2.4 Conclusions

In summary, it can be concluded:

1) When the length of graphene ribbon is much larger than L_{cr}, the rippling energy is dominant and strong enough to drive self-rippling with nonlinear periodic mode of small wavelength.

2) When the length of graphene ribbon is comparable or smaller than L_{cr}, the rippling energy cannot drive self-rippling, and an additional compressive force is needed for traditional compressed buckling of the short ribbon with the classical linear bucking mode.

3) The above estimated critical lengths (a few nanometers), are roughly consistent with some known references such as (Thompson-Flagg et al, 2009) in which only graphene samples of length larger than 20 nm could show significant self-rippling.

4) For both clamped and hinged boundary conditions, the amplitude of buckling mode driven by the rippling energy is insensitive to the length when the graphene ribbon has a length more than 1.5-2 times the critical length L_{cr}.

5) The amplitude depends on boundary constrains, which means that boundary effect cannot be ignorable for the buckling behavior of short graphene ribbons.

3.3 Substrate effect on the ripple formation

Since single-layer graphene sheets are usually mechanically exfoliated on an amorphous substrate (Bao et al, 2009), the van der Waals interaction between graphene and substrate plays a critical role in determining the morphology of

supported graphene. Recently, ultra-flat graphene was reported on Mica substrate (Lui et al, 2009) and hexagonal boron nitride substrate (Xue et al, 2011), respectively. Motivated by this, the effect of substrate on ripple formation can be studied based on the rippling energy expression (2.2).

3.3.1 Formulation

The key point here is to determine the free energy of van der Waals interaction between a rippled graphene monolayer and a rigid flat substrate. Here, the classic form of Lennard-Jones potential for the pair-wise interaction between a carbon atom and a substrate atom is taken,

$$W_{LJ}(r) = -\frac{C_1}{r^6} + \frac{C_2}{r^{12}}, \tag{3.24}$$

where r is the distance between two atoms, C_1 and C_2 are the constants for the attractive and repulsive interactions. Assuming a homogeneous substrate, we sum (integrate) the energy between one carbon atom and all the atoms in the substrate to obtain an atom-surface potential for each carbon atom near the surface. Next, summing up the atom-surface potential for all the carbon atoms in the monolayer graphene results in the monolayer-surface interaction energy. Based on this, the van der Waals free energy between a flat graphene monolayer and a rigid flat substrate can be given in the form (Aitken et al, 2010)

$$U_{wdW}(h) = -\Gamma_0[\frac{3}{2}(\frac{h_0}{h})^3 - \frac{1}{2}(\frac{h_0}{h})^9], \tag{3.25}$$

where U_{wdW} is the monolayer-surface interaction energy per unit area, h is the point-wise distance between the flat monolayer and the rigid flat substrate, h_0 is the corresponding equilibrium distance, and Γ_0 is the interfacial adhesion energy per unit area.

Assuming a rippled graphene on the substrate is in form of $h(x) = h_0 + A\sin(mx)$, (see Fig. 3.3) for a relatively small amplitude ($\frac{A}{h_0} = 1$), the average interaction energy per unit area between a rippled graphene and a rigid flat substrate is approximately given by using the 4th order Taylor expansion of $h(x)$ (Aitken et al, 2010)

$$\dot{U}_{wdW} \approx \Gamma_0(-1+\frac{27}{4}(\frac{A}{h_0})^2+\frac{675}{8}(\frac{A}{h_0})^4), \tag{3.26}$$

With the rippling energy (2.2) and the interaction energy (3.26), the total potential energy (per unit length) of a graphene ribbon with width b is

$$\begin{aligned}\dot{U}_{total} &= \frac{EI}{2}A^2m^4(1+\frac{1}{4}A^2m^2)-\mu A^2m^2(1-\gamma A^2)\\ &+\Gamma_0 b(-1+\frac{27}{4}(\frac{A}{h_0})^2+\frac{675}{8}(\frac{A}{h_0})^4),\end{aligned} \tag{3.27}$$

Minimizing Eq. (3.27) with respect to both A^2 and m^2 gives two conditions:

$$\begin{cases}\frac{EI}{2}m^4+\frac{EI}{4}A^2m^6-\mu m^2+2\mu\gamma A^2m^2+\frac{27\Gamma_0 b}{4h_0^2}+\frac{675\Gamma_0 bA^2}{4h_0^4}=0, & (3.28a)\\ EIm^2+\frac{3EI}{8}A^2m^4-\mu+\mu\gamma A^2=0. & (3.28b)\end{cases}$$

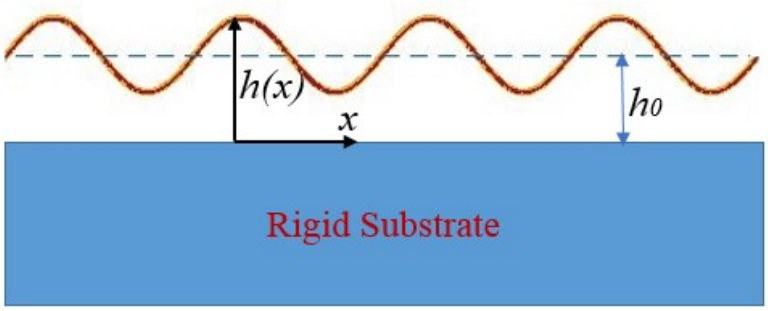

Fig. 3.3 Schematic illustration for a rippled graphene on a flat surface

3.3.2 Result on two specific substrates

For example, the equilibrium distance h_0 and the interfacial adhesion energy Γ_0 for a graphene monolayer on a mica substrate (Lui et al, 2009) are given in (Rudenko et al, 2011)

$$graphene\,on\,mica: h_0 \approx 0.49\,nm,\ \Gamma_0 \approx 4.6\,eV/nm^2 \tag{3.29}$$

Similarly, for a graphene monolayer on an hBN substrate (Xue et al, 2011), h_0 and Γ_0 are given in (Sachs et al, 2011)

$$graphene\,on\,hBN: h_0 \approx 0.35nm,\ \Gamma_0 \approx 3.8\,eV/nm^2 \tag{3.30}$$

For μ and γ within the range given in (2.19), and $EI = b \times 1\,eV$. Eqs. (3.28a) and (3.28b) can be solved easily. The results show that for both substrates the solution gives $A^2 < 0$, which means that intrinsic ripples in free-standing graphene monolayer can be fully suppressed by the mica or hBN substrate. This conclusion is consistent with known experiments (Lui et al, 2009 and Xue et al, 2011).

3.3.3 Effect of varying distance between graphene and substrate

Certainly, the values of h_0 and Γ_0 change with different substrates. Thus, the dependence of substrate effect on different substrates is a subject of great interest. Now let us study the effect on ripple formation of varying distance between the graphene monolayer and substrate. To isolate the effect of varying distance, we treat the interfacial adhesion energy Γ_0 as a given value while the distance *h* between the graphene monolayer and substrate as a variable. From Eq. (3.28b), we have

$$A^2 = \frac{\mu - EIm^2}{\frac{3EI}{8}A^2m^4 + \mu\gamma} \tag{3.31}$$

Substituting Eq. (3.31) into Eq. (3.28a), we find

$$\begin{aligned} &-\frac{E^2I^2}{16}m^8 - \frac{EI}{8}\mu m^6 + (\frac{81\Gamma_0 bEI}{32h^2} - \frac{3}{2}\mu\gamma EI)m^4 \\ &+(\mu^2\gamma - \frac{675\Gamma_0 bEI}{4h^2})m^2 + \frac{27\Gamma_0 b}{4h^2}\mu\gamma + \frac{675\Gamma_0 b\mu}{4h^2} = 0, \end{aligned} \tag{3.32}$$

Combining with Eqs. (3.31) and (3.32), the relation between the amplitude of ripple mode and the distance between graphene and substrate can be obtained easily. For example, If we choose $\mu / b = 0.427(Jm^{-2}), \gamma = 1.3\times10^{18}(m^{-2})$ $h_0 = 0.35nm,\ \Gamma_0 = 3.8\,eV/nm^2$ and $EI = b\times1\,eV$, the relation between the amplitude and the dimensionless distance (h / h_0) is given as below.

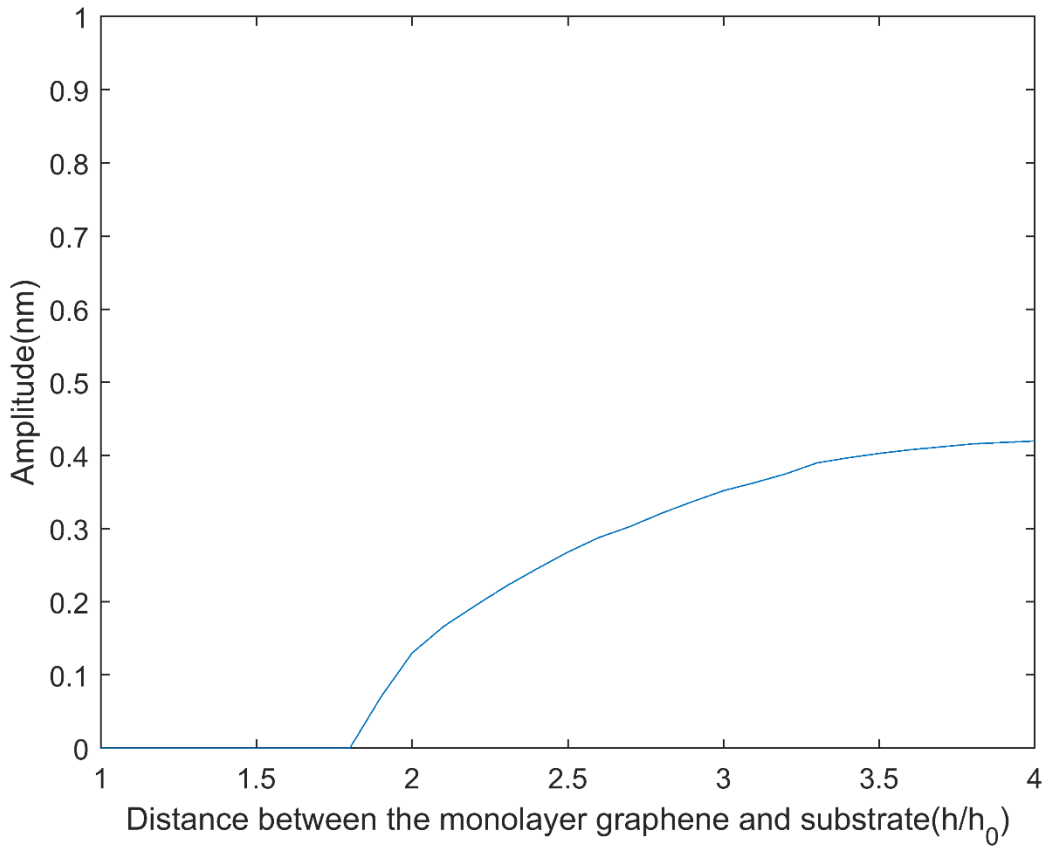

Fig. 3.4 The amplitude of ripple mode as a function of varying distance between the graphene monolayer and substrate

It is seen from Fig. 3.4 that there exists a critical distance ratio h / h_0 around 1.8 below which the van der Waals interaction is strong enough to fully suppress the ripples. Thus, the intrinsic ripples in graphene monolayer cannot exist when the distance between graphene and substrate is smaller than this critical value. However, the van der Waals energy will decrease with increasing distance. Therefore, the ripples start to appear when the distance ratio h / h_0 is bigger than 1.8 and the amplitude of ripple mode is

growing fast with the increasing distance. When the distance ratio h / h_0 is bigger than 4, it is seen from Fig.3.4 that the van der Waals interaction can be ignored and the graphene monolayer can be treated approximately as a free-standing graphene.

3.3.4 Conclusions

In summary, it can be concluded:

1) In the appearance of a rigid substrate, the intrinsic ripples in free-standing graphene monolayer tends to be suppressed by the van der Waals interaction between the substrate and graphene. For some specific substrates, such as mica or hBN. The ripples can be fully suppressed at the equilibrium distance between graphene and substrate.

2) There exists a critical distance between graphene and substrate. When the distance is smaller than the critical distance, ripples in graphene monolayer cannot exist due to the strong van der Waals interaction. However, when the distance is several times larger than the critical distance. the effect of substrate can be ignored and the graphene monolayer can be treated approximately as a free-standing graphene.

Chapter 4

Conclusions and future work

4.1 Conclusions

Several candidate phenomenological expressions are studied for self-rippling energy that drives ripple formation of free single-layer graphene sheets. One phenomenological expression is admitted, while all others are rejected because they cannot admit stable periodic ripple mode. The admitted phenomenological expression contains two terms: one quadratic term which acts like a compressive force and has a destabilizing effect and another fourth-order term which acts like a nonlinear elastic foundation and has a stabilizing effect. Between the two coefficients one of the proposed expression is largely determined by the wavelength but insensitive to the amplitude of ripple mode, while the other one is essentially determined by the amplitude but insensitive to the wavelength. The two associated coefficients depend on specific mechanism of self-rippling and can be determined based on observed wavelength and amplitude of ripple mode. Based on the admitted expression, some application of the proposed model are examined. The major conclusions are summarized below:

1) The effect of an applied force on ripple formation is studied. Our model show that with an applied tensile force, ripples can be controlled or even fully suppressed. This conclusion is consistent with relative references, the minimum tensile strain to eliminate rippling is determined by the coefficient μ, and is about 0.06%-0.26%. In particular, if

the wavelength of free rippling mode is around 6 nm, the minimum tensile strain given by the present model is about 0.16%, in remarkable agreement with known related data 0.25% where the wavenumber of free rippling is around 1/nm (which corresponds to a wavelength of $\approx 6nm$). On the other hand, under a sufficient compressive stress, the present model predicts that ripples would be collapsed into narrow standing wrinkles of minimum wavelengths around 2.2 nm, reasonably consistent with some observed minimum wavelength 2 nm.

2) Our results show that self-rippling energy dominates ripple formation of sufficiently long free graphene ribbons, although it cannot drive self-rippling of sufficiently short free graphene ribbons. Consequently, a critical length is estimated so that self-rippling occurs only when the length of free single-layer graphene ribbons is much longer than the critical length. The estimated critical length is reasonably consistent with the known fact that self-rippling cannot occur in shorter free graphene sheets (say, of length below 20 nm). Further, the effect of rippling energy on traditional compressed buckling of short graphene ribbons is examined. The results show that initial post-buckling of traditional half-wave or single-wave buckling mode can exist for short graphene ribbons, while multi-wave ripple mode occurs only for sufficiently long graphene ribbons. It is expected that the proposed phenomenological model could be used to study other rippling-related mechanical behavior of graphene ribbons.

3) Finally, the effect of a rigid substrate on ripple formation has been studied, and the results show that the rippling can be suppressed and the graphene monolayer can be ultra-flat in the appearance of a rigid substrate due to the van der Waals interaction

between the substrate and graphene. There exists a critical value of distance below which ripples in graphene monolayer cannot exist due to the strong van der Waals interaction. However, when the distance is several times larger than the critical distance. the effect of substrate can be ignored and the graphene monolayer can be treated approximately as a free-standing graphene.

4.2 Future work

In the thesis, we treat the graphene as a 1D elastic beam or ribbon. A 2D model for rippling energy of free-standing graphene membranes could be developed based on the present model by replacing w_x by ∇w, as shown below

$$-\mu\iint_A (\nabla w \mathrm{g} \nabla w)(1-4\gamma w^2)ds \tag{4.1}$$

Further details would be investigated in a future work.

Bibliography

Aitken Z. H., Huang R.,” Effects of mismatch strain and substrate surface corrugation on morphology of supported monolayer graphene.” J. Appl. Phys.107, 12 (2010).

Amorim B., Cortijo A., de Juan F., Grushin A. G., Guinea F., Gutiérrez-Rubio A., Ochoa H., Parente V., Roldán R., San-José P., Schiefele J., Sturla M., and H. Vozmediano M. A., “Novel effects of strains in graphene and other two dimensional materials”Phys. Rep. 617(1) (2016).

Bai K. K., Zhou Y., Zheng H., Meng L., Peng H., Liu Z., Nie J. C., and He L., Creating one-dimensional nanoscale periodic ripples in a continuous mosaic graphene monolayer, Phys. Rev. Lett. 113, 086102 (2014).

Balandin A. A.. “Thermal properties of graphene and nanostructured carbon materials”. Nature Mater. 10, 569 (2011)

Bangert , U. Gass , M. H. Bleloch A. L., Nair R. R., and Geim A. K., “Manifestation of ripples in free-standing graphene in lattice images obtained in an aberration-corrected scanning transmission electron microscope,” Phys. Status Solidi A 206, 1117 (2009)

Bao W., Miao F., Chen Z., Zhang H., Jang, Dames W. C., and Lau C. N., "Controlled ripple texturing of suspended graphene and ultrathin graphite membranes," Nat. Nanotechnol. 4, 562 (2009).

Breitwieser R., Hu Y. C., Chao Y. C., Li R. J., Tzeng Y. R., Li L. J., Liou S. C., Lin K. C., Chen C. W., Pai W. W., "Flipping nanoscale ripples of free-standing graphene using a scanning tunneling microscope tip," Carbon, 77 ,236(2014).

Bunch J. S., Verbridge S. S., Alden J. S., Van Der Zande A. M., Parpia J. M., Craighead H. G., and McEuen P. L., "Impermeable atomic membranes from graphene sheets". Nano Lett. 8, 2458 (2008)

Carlsson J. M., "Graphene: buckle or break," Nature Mater. 6, 801 (2007).

Capasso A., Placidi E., Zhan H. F., Perfetto E., Bell J. M., Gu Y. T., and Motta N., "Graphene ripples generated by grain boundaries in highly ordered pyrolytic graphite," Carbon ,68, 330 (2014).

Fasolino A., Los J. H., and Katsnelson M. I., "Intrinsic ripples in graphene," Nature Mater. 6, 858 (2007).

Gao W. , and Huang R., " Thermomechanics of monolayer graphene: Rippling, thermal expansion and elasticity," J. Mech. Phys. Solids, 66, 42 (2014).

Hunt G. W., Wadee M. K., and Shiacolas N., "Localized elasticae for the strut on the linear foundation," ASME J. Appl. Mech. 60, 1033 (1993).

Khamlichi A., Elbakkali L., and Limam A., "Postbuckling of elastic beams considering higher order strain terms," J. Eng. Mech. 127, 372 (2001).

Lee S., "Effect of Intrinsic Ripples on Elasticity of the Graphene Monolayer." Nanoscale Res. Lett., 10, 422 (2015).

Lee C. , Wei X., Kysar J. W., and Hone J., "Measurement of the elastic properties and intrinsic strength of monolayer graphene". Science. 387, 385(2008)

Lindahl N., Midtvedt D., Svensson J. , Nerushev O. A., Lindvall N., Isacsson A. , and Campbell E. E., "Determination of the bending rigidity of graphene via electrostatic actuation of buckled membranes," Nano lett. 12, 3526(2012).

López-Polín G., Jaafar M. , Guinea F., Roldán R. , Gómez-Navarro C. , and Gómez-Herrero J., "Strain dependent elastic modulus of graphene".arXiv preprint arXiv:1504.05521(2015)

Lui C. H., Liu L., Mak K. F., Flynn G. W., and Heinz T. F., "Ultraflat graphene,"Nature. 462, 339 (2009).

Mayorov A. S., Gorbachev R. V., Morozov S. V., Britnell L., Jalil R., Ponomarenko L. A., Blake P., Novoselov K. S., Watanabe K., Taniguchi T., and Geim A. K.. "Micrometer-scale ballistic transport in encapsulated graphene at room temperature". Nano Lett. 11, 2396 (2011)

Mermin N. D.. "Crystalline order in two dimensions". Physical Review, 176,1(1968).

Meyer J. C., Geim A. K., Katsnelson M. I., Novoselov K. S., Booth T. J., and Roth S., "The structure of suspended graphene sheets," Nature 446, 60 (2007).

Moser J., Barreiro A., and Bachtold A.. "Current-induced cleaning of graphene". Appl. Phys. Lett. 91, 163513 (2007)

Mounet N., and Marzari N., "First-principles determination of the structural, vibrational and thermodynamic properties of diamond, graphite, and derivatives," Phys. Rev. B, 71, 205214(2005)

Nair R. R., Blake P., Grigorenko A. N., Novoselov K. S., Booth T. J., Stauber T., Peres N. M., and Geim A. K.. "Fine structure constant defines visual transparency of graphene". Science 320, 1308 (2008)

Novoselov K. S., Geim A. K., Morozov S. V., Jiang D., Zhang Y., Dubonos S. V., Grigorieva I. V. , and Firsov A. A.. "Electric field effect in atomically thin carbon films". science, 306, 5696 (2004)

Pereira V. M., Neto A. C., Liang H. Y. , and Mahadevan L., "Geometry, mechanics, and electronics of singular structures and wrinkles in graphene." Phys. Rev. Lett.105, 156603(2010).

Roldán R., Fasolino A., Zakharchenko K. V., and Katsnelson M. I., "Suppression of anharmonicities in crystalline membranes by external strain" Phys. Rev. B. 83, 17 (2011)

Rudenko A. N., Keil F. J., Katsnelson M. I., and Lichtenstein A. I.," Graphene adhesion on mica: Role of surface morphology" Phys. Rev. B 83, 045409 (2011).

Ru C.Q., "Ripple formation of free graphene ribbons driven by self-attractive forces," Appl Phys Lett, 103, 043104(2013).

Sachs B., Wehling T. O., Katsnelson M. I., and Lichtenstein A. I.," Adhesion and electronic structure of graphene on hexagonal boron nitride substrates" Phys. Rev. B 84, 195414 (2011).

Thompson-Flagg R. C., Moura M. J. B., and Marder M., "Rippling of graphene," Europhys. Lett. 85, 46002 (2009).

Wang W. L., Bhandari S., Yi W., Bell D. C., Westervelt R., and Kaxiras E., "Direct imaging of atomic-scale ripples in few-layer graphene,"Nano Lett. 12, 2278 (2012)

Xue J., Sanchez-Yamagishi J., Bulmash D., Jacquod P., Deshpande A., Watanabe K., Taniguchi T., Jarillo-Herrero P., and LeRoy B. J., "Scanning tunnelling microscopy

and spectroscopy of ultra-flat graphene on hexagonal boron nitride," Nat. Mater. 10, 282 (2011)

Yoon D., Son Y. W., and Cheong H., "Negative thermal expansion coefficient of graphene measured by Raman spectroscopy." Nano lett. 11,3227(2011)

Zan R., Muryn C., Bangert U., Mattocks P., Wincott P., Vaughan D., Li X., Colombo L., Ruoff R. S., Hamilton B., and Novoselov K.S., "Scanning tunnelling microscopy of suspended graphene," Nanoscale 4, 3065 (2012).

Zhang K., and Arroyo M., "Understanding and strain-engineering wrinkle networks in supported graphene through simulations," J. Mech. Phys. Solids, 72,61 (2014).

Zhu W., Low T., Perebeinos V., Bol A. A., Zhu Y., Yan H., Tersoff J., and Avouris P., "Structure and electronic transport in graphene wrinkles," Nano Lett. 12, 3431 (2012)